



Minimizing the effects of Pb loss in detrital and igneous U–Pb zircon geochronology by CA-LA-ICP-MS

Erin E. Donaghy¹, Michael P. Eddy¹, Federico Moreno², and Mauricio Ibañez-Mejía²

¹Department of Earth, Atmospheric, and Planetary Sciences, Purdue University, West Lafayette, IN 47907, United States of America

²Department of Geosciences, University of Arizona, Tucson, AZ 85721, United States of America

Correspondence: Erin E. Donaghy (edonaghy@purdue.edu)

Received: 20 July 2023 – Discussion started: 25 August 2023

Revised: 24 January 2024 – Accepted: 29 January 2024 – Published: 27 March 2024

Abstract. Detrital zircon geochronology by laser ablation–inductively coupled plasma–mass spectrometry (LA-ICP-MS) is a widely used tool for determining maximum depositional ages and sediment provenance, as well as reconstructing sediment routing pathways. Although the accuracy and precision of U–Pb geochronology measurements have improved over the past 2 decades, Pb loss continues to impact the ability to resolve zircon age populations by biasing affected zircon toward younger apparent ages. Chemical abrasion (CA) has been shown to reduce or eliminate the effects of Pb loss in zircon U–Pb geochronology but has yet to be widely applied to large-*n* detrital zircon analyses. Here, we assess the efficacy of the chemical abrasion treatment on zircon prior to analysis by LA-ICP-MS and discuss the advantages and limitations of this technique in relation to detrital zircon geochronology. We show that (i) CA does not systematically bias LA-ICP-MS U–Pb dates for 13 reference materials that span a wide variety of crystallization dates and U concentrations, (ii) CA-LA-ICP-MS U–Pb zircon geochronology can reduce or eliminate Pb loss in samples that have experienced significant radiation damage, and (iii) bulk CA prior to detrital zircon U–Pb geochronology by LA-ICP-MS improves the resolution of age populations defined by $^{206}\text{Pb}/^{238}\text{U}$ dates (Neoproterozoic and younger) and increases the percentage of concordant analyses in age populations defined by $^{207}\text{Pb}/^{206}\text{Pb}$ dates (Mesoproterozoic and older). The selective dissolution of zircon that has experienced high degrees of radiation damage suggests that some detrital zircon age populations could be destroyed or have their abundance significantly modified during this process. However, we did not identify this effect in either of the de-

trital zircon samples that were analyzed as part of this study. We conclude that pre-treatment of detrital zircon by bulk CA may be useful for applications that require increased resolution of detrital zircon populations and increased confidence that $^{206}\text{Pb}/^{238}\text{U}$ dates are unaffected by Pb loss.

1 Introduction

Detrital zircon U–Pb geochronology is a widely used tool with a broad range of applications across multiple subdisciplines of geology. As the efficiency, accuracy, and precision of U–Pb geochronology measurements continue to improve (e.g., Carrapa, 2010; Gehrels, 2012, 2014; Pullen et al., 2014; Sundell et al., 2021), the production of large detrital zircon datasets by laser ablation–inductively coupled plasma–mass spectrometry (LA-ICP-MS) has become more common. In basin analysis and tectonics, these datasets are often used to determine sediment provenance, characterize source terranes, estimate maximum depositional ages, and reconstruct ancient sediment routing pathways (Fedo et al., 2003; Anderson, 2005; Smith et al., 2023). The resulting data are typically interpreted using kernel density estimates (KDEs) or probability density plots (PDPs) and assessed by comparing the means, heights, widths, and modes of peaks in detrital zircon age spectra using similarity and dissimilarity metrics. One factor that may limit the resolution of these peaks is Pb loss, which can smear zircon age populations toward younger apparent U–Pb dates. This issue may not bias data in which Pb loss is a recent phenomenon provided that the $^{207}\text{Pb}/^{206}\text{Pb}$ date is used for zircon crystalliza-

tion. However, protracted or complicated histories of Pb loss can make it difficult to interpret $^{207}\text{Pb}/^{206}\text{Pb}$ dates (Nemchin and Cawood, 2005), and many labs only use this system to constrain a zircon crystallization date if it is concordant. The precision of the $^{207}\text{Pb}/^{206}\text{Pb}$ chronometer also typically limits its use to Mesoproterozoic and older zircon. The most precise date for Neoproterozoic or younger zircon is generally obtained with the $^{206}\text{Pb}/^{238}\text{U}$ chronometer, and these dates are more susceptible to open-system behavior. Zircon age populations that are affected by Pb loss in this age range can be difficult to identify since Pb loss trajectories closely follow concordia and may result in analyses that are concordant within analytical uncertainty but have spuriously young $^{206}\text{Pb}/^{238}\text{U}$ dates. This is especially problematic for the estimation of maximum depositional ages (MDAs) in detrital zircon datasets where age estimations utilize low- n clusters of the youngest zircon ages (Dickinson and Gehrels, 2009; Herriott et al., 2019; Coutts et al., 2019; Sharman and Malkowski, 2020; Vermeesch, 2021). The effect of Pb loss on detrital zircon analyses is consequently twofold. It reduces the number of concordant Mesoproterozoic and older zircons, making populations in this age range more difficult to identify, and it will cryptically smear Neoproterozoic and Phanerozoic zircon age populations along concordia toward spuriously young dates, making it difficult to resolve differences between distinct but similarly aged populations.

While high-temperature metamorphism may lead to zircon recrystallization and partial, or total, resetting of the U–Pb system, most Pb loss in zircon that is hosted in sedimentary strata represents a low-temperature process. Damage to the zircon crystal lattice occurs during each alpha emission along the ^{238}U , ^{235}U , and ^{232}Th decay chains as the heavy nucleus recoils (Bateman, 1910; Dickin, 2005; Nasdala et al., 2005; Reiners, 2005). At temperatures below 200 °C this damage cannot anneal and begins to accumulate (Marsellos and Garver, 2010; Ginster et al., 2019). Areas where high levels of damage have accumulated are then susceptible to Pb loss (Chakoumakos et al., 1987; Mattinson, 1994; Garver and Kamp, 2002; Widmann et al., 2019; McKenna et al., 2023). The mechanisms through which Pb becomes mobile in metamict zircon grains remain understudied but likely include mobility in low-temperature aqueous fluids (Goldich and Mudrey, 1972; Black, 1987; Kramers et al., 2009; Keller et al., 2019), which allows water to penetrate highly radiation-damaged zircon and mobilize radiogenic Pb by changing its redox state (Kramers et al., 2009). Thus, the zircons that are most susceptible to Pb loss at low temperatures are those that spend long durations at shallow crustal levels and encounter low-temperature aqueous fluids, both of which are conditions seen by detrital zircon hosted in sedimentary basins.

The chemical abrasion method, in which thermally annealed zircon is partially dissolved in hydrofluoric acid (HF) prior to analysis, has been shown to successfully mitigate low-temperature Pb loss (e.g., Mundil et al., 2004;

Mattinson, 2005; Widmann et al., 2019; Sharman and Malkowski, 2023) and is widely used in isotope dilution–thermal ionization–mass spectrometry (ID-TIMS) U–Pb zircon geochronology (see reviews in Schoene, 2014; Schaltegger et al., 2015). The technique likely benefits analyses in two ways. First, it selectively dissolves zones of the zircon crystal that have experienced extensive radiation damage and possible Pb loss (Widmann et al., 2019; McKenna et al., 2023). Second, the partial dissolution process dissolves inclusions that may harbor non-radiogenic Pb, leading to a higher proportion of zircon-hosted radiogenic Pb (Pb^*) in the measured analysis. Over the last decade, several groups have analyzed chemically abraded zircon by LA-ICP-MS and shown that this approach can successfully mitigate Pb loss and results in increased concordance, precision, and, presumably, accuracy of U–Pb dates (Crowley et al., 2014; Von Quadt et al., 2014). These results suggest that chemical abrasion prior to large- n detrital zircon analyses may also be useful when the resolution of closely spaced Neoproterozoic and Phanerozoic peak age populations is desired or when high degrees of discordance obscure the interpretation of Mesoproterozoic and older age populations. Here, we assess the benefits and drawbacks of this pre-treatment with a particular focus on whether the resolution of younger zircon age populations is increased, whether it improves concordance for Precambrian detrital zircon populations, and/or whether the selective removal of metamict zircon will bias age populations.

2 U–Pb zircon geochronology approach and methods

We have divided our study into three distinct parts. First, we compare chemically abraded and untreated zircon from 13 zircon reference materials (Table 1) to test whether chemical abrasion systematically biases U–Pb dates analyzed by LA-ICP-MS. Crowley et al. (2014) demonstrated that chemically abraded zircon ablates more slowly and experiences greater down-hole fractionation than untreated zircon. These differences are likely related to changes in the ability of the laser to couple with zircon that has been etched by the chemical abrasion process. While no negative effects of chemical abrasion were seen in Crowley et al. (2014) or von Quadt et al. (2014), provided that chemically abraded reference materials were used for instrument calibration, we have expanded the age range of reference zircon analyzed to encompass 28.5–3467 Ma. This increased age range of the tested reference materials provides a more complete understanding of LA-ICP-MS U–Pb systematics on chemically abraded zircon and whether a single primary reference material can be used to calibrate the instrument for a wide range of zircon dates. Second, we assess the ability of chemical abrasion to mitigate Pb loss in an igneous sample that has experienced substantial radiation damage by comparing chemically abraded and non-

chemically abraded $^{206}\text{Pb}/^{238}\text{U}$ LA-ICP-MS zircon analyses to a newly produced CA-ID-TIMS reference date for a Mesoproterozoic granite. Finally, we assess how CA affects detrital zircon (DZ) age spectra by comparing chemically abraded and untreated aliquots of two detrital samples. One sample is Cenozoic in age and contains both Phanerozoic (100–300 Ma) and Precambrian (1000–1200 Ma) zircon age populations, whereas the second sample is Proterozoic and contains zircon age populations between 2000 and 3500 Ma.

2.1 Methods for thermal annealing and chemical abrasion

All chemically abraded zircon aliquots were treated at Purdue University following methods modified from Mattinson (2005) and similar to those described in Eddy et al. (2019). Zircon separates were first thermally annealed in quartz crucibles for 60 h at 900 °C in a muffle furnace and then loaded in 3 mL Savillex hex beakers with ~1 mL of 28 M HF and 0.1 mL of 8 M HNO₃ for bulk chemical abrasion. Four hex beakers were then stacked in the PTFE liner for a 125 mL Parr acid dissolution vessel. To ensure vapor exchange during partial dissolution a small hole was drilled through each beaker cap. The fully assembled Parr acid dissolution vessel was then held at 210 °C for 12 h. Once the chemical abrasion process was completed, the leachate was removed from each beaker using a pipette and the zircons were rinsed three times with H₂O. Chemically abraded aliquots were then sent to the University of Arizona Laser-Chron Center (ALC) for mounting and LA-ICP-MS analyses. Methods for chemical abrasion of zircon prior to the ID-TIMS analyses reported in this paper are similar to those described above, except individual zircons were chemically abraded in 200 μL Ludwig-style microcapsules and repeatedly rinsed in distilled 7 M HCl and ultrapure H₂O prior to spiking and complete dissolution.

2.2 LA-ICP-MS zircon U–Pb geochronology

Zircon aliquots were mounted in 2.5 cm diameter epoxy plugs, polished, and imaged by cathodoluminescence using a Hitachi 3400N SEM and a Gatan Chroma CL system prior to analysis by LA-ICP-MS. Chemically abraded zircons were only mounted with chemically abraded zircon reference materials, while untreated zircon aliquots were mounted with untreated reference materials. U–Pb isotopic analyses were obtained via LA-ICP-MS using a Thermo Element2 single-collector ICP-MS coupled with a Teledyne Photon Machines Analyte G2 excimer laser at the ALC. The diameter of the laser spot was set to 30 μm . Elemental- and mass-dependent instrumental fractionation was corrected by bracketing unknown analyses with analyses of primary reference material FC1 following the methods described in Pullen et al. (2018). Please see Table S23 in the Supplement for tuning parameters for the laser and mass spectrometer. Only chemically

abraded primary reference materials were used for calibration of chemically abraded samples and only untreated primary reference materials were used for untreated samples following the recommendations of Crowley et al. (2014). Bracketing of secondary and tertiary reference materials occurred every 10–11 analyses with primary reference materials (FC1, SLF/SLM, R33) for the round-robin comparison of zircon reference materials, every 2–3 analyses for igneous zircon analyses, and every 5 analyses for detrital zircon samples. Data reduction was completed using an in-house MATLAB script, AgeCalcML v.1.42 (Sundell et al., 2021). This program allows the user to filter data by maximum $^{206}\text{Pb}/^{238}\text{U}$ and/or $^{207}\text{Pb}/^{206}\text{Pb}$ uncertainty (typically set to 10 %), reverse discordance (typically 5 %), and normal discordance (typically 20 %). For the purposes of this study, we deactivated all uncertainty and discordance filters in AgeCalcML and all isotopic data measured via LA-ICP-MS that are clearly from ablated zircon are reported in Tables S1–S13. However, age interpretations of igneous and detrital zircon data use filtered data (Tables S16–S21).

Uranium concentrations (ppm) reported from routine U–Pb LA-ICP-MS zircon analyses at ALC are semiquantitative and calibrated by bracketing unknowns with analyses of reference materials with a known average U concentration. However, since chemical abrasion selectively dissolves high-uranium zones and thus modifies the average U concentration of reference materials by an unquantified amount, the reported U concentration values for reference materials analyzed by traditional (non-CA) ID-TIMS may no longer be valid. We found that the primary reference material SLF had homogenous ^{238}U cps (counts per second) within individual sessions (Figs. S15–S17 in the Supplement) for both the CA and non-CA runs. We interpret this to mean that SLF has a homogenous U concentration (and radiation damage) and that any differences in ^{238}U cps for SLF between different analytical sessions are related to changes in the instrument's sensitivity. As such, we normalize the ^{238}U cps for all other grains analyzed in each session to the average ^{238}U cps of SLF across all sessions. Given the potential difference between chemically abraded and untreated SLF U concentrations, we did this correction independently for treated and untreated grains. Since we do not have U concentration values for treated and untreated SLF, we center our discussions on relative differences in U concentration as estimated using the intensity (in cps) of the ^{238}U beam rather than quantifying U concentrations.

We used the Saylor and Sundell (2016) DZstats program to complete a quantitative assessment of the similarity between treated and untreated aliquots. This program implements five tests to compare large-*n* geochronologic or thermochronologic datasets. The tests used in this study are similarity, likeness, and cross-correlation. Results from all five tests are shown in Table S22 for both detrital zircon samples. The similarity coefficient measures if two samples have similar modal sub-intervals as well as similar proportions of

Table 1. Zircon reference materials for U–Pb isotopic analyses.

Name	ID-TIMS age (Ma)	2σ	References	Host lithology	Quantity
Fish Canyon Tuff	28.476	0.029	Schmitz and Bowring (2001) ^{b,c}	Dacite	Unlimited
GHR1	48.106	0.023	Eddy et al. (2019) ^b	Rapakivi granite	Unlimited
49127	136.6		Gehrels et al. (2008) ^b		Uncertain
Plesovice	337.13	0.37	Sláma et al. (2008) ^a	Potassic granulite	Unlimited
Temora 2	418.37	0.14	Mattinson (2010) ^a	Gabbro	Unlimited
R33	420.53	0.16	Mattinson (2010) ^a	Monzodiorite	Unlimited
SLM	563.5	3.2	Gehrels et al. (2008) ^b	Single crystal	Limited
SLF	555.86	0.68	Wang et al. (2022) ^b	Single crystal	Limited
91500	1065.4	0.3	Wiedenbeck et al. (1995) ^b	Single crystal	Limited
FC1	1098.47	0.16	Mattinson (2010) ^a	Gabbro	Unlimited
Oracle	1434	8	Gehrels et al. (2008) ^b	Granite	Unlimited
QGNG	1851.6	0.6	Black et al. (2004) ^b	Quartz gabbro gneiss	Uncertain
OG1	3467.05	0.63	Stern et al. (2009) ^a	Diorite	Unlimited

^a Chemical abrasion CA-ID-TIMS. ^b Traditional ID-TIMS. ^c CA-ID-TIMS analyses by Wotzlaw et al. (2013) show significant age dispersion in Fish Canyon Tuff relative to original U–Pb ID-TIMS dates of Schmitz and Bowring (2001).

components in each one of those modes. A value for similarity equal to 1 indicates the samples are identical in both peak modes and proportions, whereas 0 indicates there is no match between modes and proportions (Saylor and Sundell, 2016). This test is useful in assessing the number of peak age populations (similar mode intervals) and how peak heights (proportion of components in each mode) change between two samples. The cross-correlation coefficient is also sensitive to the presence or absence of peak ages but also changes due to the relative magnitude and shape of peaks. If a sample shared the same peak ages, peak shapes, and magnitude of peaks, it would have an R^2 value of 1. If no peak ages, peak shapes, and magnitude of peaks are shared, the R^2 value would be 0 (Saylor and Sundell, 2016). Likeness is the complement of the area of mismatch between two detrital zircon spectra, or more simply put the degree of “sameness” between detrital zircon age populations (Satkoski et al., 2013). Thus, the likeness test compares the degree of overlap between pairs of PDPs and is a measure of resemblance between proportions of two populations with overlapping ages (Gehrels et al., 2009; Satkoski et al., 2013). Values of likeness that approach 1 indicate that two detrital zircon spectra have a high degree of overlap (Satkoski et al., 2013; Saylor and Sundell, 2016).

2.3 Zircon optical profilometry

To evaluate the effect of CA on laser ablation excavation rates in zircons, we compared the average depth at increasing ablation times on a series of laser pits on treated and untreated reference materials. This was accomplished by generating 10 laser ablation pits with excavation times that increased by 3 s (starting at 3 and increasing to 30 s) in single crystals of treated and untreated grains of zircon reference materials FC1, R33, and SL. The resulting pits were imaged using a

Veeco Wyko NT9800 optical profilometer, and depth maps, 3-D images, and crosscut profiles were created using the Vision software produced by Veeco. The images and profiles allowed for the estimation of pit depths and can be used to calculate excavation rates when combined with the known ablation periods (Fig. 2). Laser ablation pits were also imaged and measured on three treated and five untreated unknowns from sample MIGU-02.

2.4 CA-ID-TIMS zircon U–Pb geochronology

Sample MIGU-02, a granitoid from the Guiana Shield, was analyzed by CA-ID-TIMS at Purdue University to provide a reference date to compare the chemically abraded and untreated LA-ICP-MS analyses. Following the chemical abrasion methods described above, individual zircons were spiked with the EARTHTIME ^{205}Pb – ^{233}U – ^{235}U isotopic tracer (Condon et al., 2015; McLean et al., 2015) and loaded into a Parr acid digestion vessel with 28 M HF. The vessel was then held at 210 °C for 60 h for zircon dissolution. After dissolution, the samples were dried down and converted to chloride form by adding 75 μL 7 M HCl, reassembling the Parr acid digestion vessel, and holding it at 180 °C for 12 h. After conversion to chloride form, the solution was converted to 3 M HCl in preparation for anion exchange chromatography. Pb and U were purified from these solutions using AG-1x8 anion exchange resin following procedures modified from Krogh (1973). The resulting aliquots were dried down to a chloride salt before being dissolved in silica gel, dried onto rhenium filaments, and loaded into an IsotopX Phoenix TIMS for analysis. Pb isotopic measurements were made by peak hopping on a Daly detector and corrected for mass-dependent isotopic fractionation using $\alpha = 0.147 \pm 0.028$ (% amu) and dead time of 29.9 ns, derived from repeat measurements of the NBS981

Pb reference material. We assume that all ^{204}Pb is from laboratory contamination and correct for it using a laboratory Pb isotopic composition of $^{206}\text{Pb}/^{204}\text{Pb} = 18.82 \pm 0.74$ (2σ), $^{207}\text{Pb}/^{204}\text{Pb} = 15.52 \pm 0.63$ (2σ), and $^{208}\text{Pb}/^{204}\text{Pb} = 37.93 \pm 1.60$ (2σ) derived from repeat total procedural blank measurements run during 2022. Uranium was run as an oxide (UO_2), and isotopic measurements were made statically using Faraday detectors and corrected for fractionation using the known ratio of $^{233}\text{U}/^{235}\text{U}$ in the EARTHTIME ^{205}Pb – ^{233}U – ^{235}U isotopic tracer (Condon et al., 2015; McLean et al., 2015) and assuming a zircon $^{238}\text{U}/^{235}\text{U}$ value of 137.818 ± 0.045 (Hiess et al., 2012). Data reduction was done using the ET_Redux software package (Bowring et al., 2011) and the decay constants of Jaffey et al. (1971). All isotopic data measured via CA-ID-TIMS are presented in Table S17.

3 Results

3.1 CA-LA-ICP-MS U–Pb geochronology of zircon reference materials

Treated and untreated aliquots of 13 different zircon U–Pb reference materials (Table 1) were analyzed in this study to further assess whether chemical abrasion systematically biases U–Pb dates. The reference materials were analyzed during two round-robin runs using the approach described above. The first run targeted 15 zircon grains from treated and untreated aliquot of reference materials. During the second run, 30 zircon grains were targeted. Because FC1 was used as a primary reference material for calibration of the LA-ICP-MS, approximately 30 FC1 zircons were analyzed during run one and 87 were analyzed during run two in both treated and untreated aliquots. This led to 117 FC1 grains analyzed per treated and untreated aliquots of reference material. The total number of zircons analyzed was 653 in each of the chemically abraded and untreated aliquots of reference materials. Of the 653 grains in the chemically abraded aliquots, 631 analyses (96.6 %) were retained following filtering for discordance, whereas 608 analyses (93.5 %) were retained in the untreated aliquot. These results further confirm that CA helps mitigate Pb loss and improve the percentage of retained concordant LA-ICP-MS analyses (e.g., Crowley et al., 2014; von Quadt et al., 2014). The most extreme change in concordance and data retention occurred between treated and untreated FC1 zircon (1098.4 Ma). Of the 117 grains analyzed in both the treated and untreated aliquots, 99.1 % of analyses were retained in the chemically abraded aliquot versus 82.2 % in the untreated aliquot. Discordance criteria used for filtering the above data were reverse discordance larger than 5 %, $^{206}\text{Pb}/^{238}\text{U}$ errors larger than 10 %, and/or maximum discordance of over 20 %. Overall, the discordant FC1 grains in both runs had low U cps and significantly older $^{206}\text{Pb}/^{238}\text{U}$ dates (> 1250 Ma; Fig. S15).

The weighted-mean dates of CA and non-CA reference materials are all within 0.1 %–4 % of the reference ages determined by ID-TIMS (Fig. 1). Therefore, despite an increase in the percent of concordant treated grains relative to untreated grains, weighted means of acceptable analyses are indistinguishable and indicate that it is unlikely that chemical abrasion biases U–Pb dates within LA-ICP-MS instrument uncertainty. The greatest scatter in calculated weighted-mean ages (~ 4 % to 0.1 % age offset from reference date) is in both the treated and untreated Mesozoic to Cenozoic reference materials. Scatter is improved by chemical abrasion in Paleozoic reference materials (2 % to 0.8 % age offset) and excellent for Proterozoic and Archean aliquots (0.6 % to -0.7 %). Additionally, concordant analyses of treated aliquots have overall lower ^{238}U cps compared to the untreated aliquots (Fig. S15), indicating that chemical abrasion dissolved zones of high U concentrations where Pb loss is most likely to have occurred (Widmann et al., 2019; McKenna et al., 2023). Since reference materials are selected for their homogeneous isotopic compositions, it is not surprising that there is similarity in dates between treated and untreated aliquots. The reproducibility of U–Pb dates for all of the reference materials is strong evidence that a single primary reference material (FC1 in this case) can be used to correct for instrumental fractionation across a wide range of zircon ages and trace element compositions for chemically abraded zircon.

Despite the overall similarity in bias between treated and untreated reference materials, the behavior of some reference materials warrants further discussion. The CA-LA-ICP-MS weighted-mean $^{206}\text{Pb}/^{238}\text{U}$ dates for two Cenozoic reference materials were older than the CA-ID-TIMS reference date. Chemical abrasion of GHR1 zircon led to an increase in concordant grains but an older $^{206}\text{Pb}/^{238}\text{U}$ weighted-mean date (Fig. S2). We attribute this difference to the presence of slightly older xenocrysts within the sample (e.g., Eddy et al., 2019). We see a similar result for Fish Canyon Tuff zircon where the CA aliquot showed increased concordance, but the calculated mean age was offset more from the reference age than the no-CA aliquot (Fig. S1). This sample contains significant antecrysts that might bias its results (e.g., Wotzlaw et al., 2013). Indeed, increased precision and accuracy in analyses of young suites of igneous zircon routinely find overdispersion that can be related to protracted zircon growth or the presence of xenocrysts and/or antecrysts. Thus, the slight variability in weighted-mean dates for GHR1 and Fish Canyon samples in CA-LA-ICP-MS analyses is not entirely unexpected and therefore unlikely to reflect a systematic bias of the CA-LA-ICP-MS method. Additionally, the 91500 reference material has shown substantial negative age offset in other studies (Gehrels et al., 2008; Schoene, 2014), but the origin of these offsets has remained enigmatic, and the offset in this study is not surprising.

Variations in laser ablation behavior between primary reference materials used for standardization and samples is a

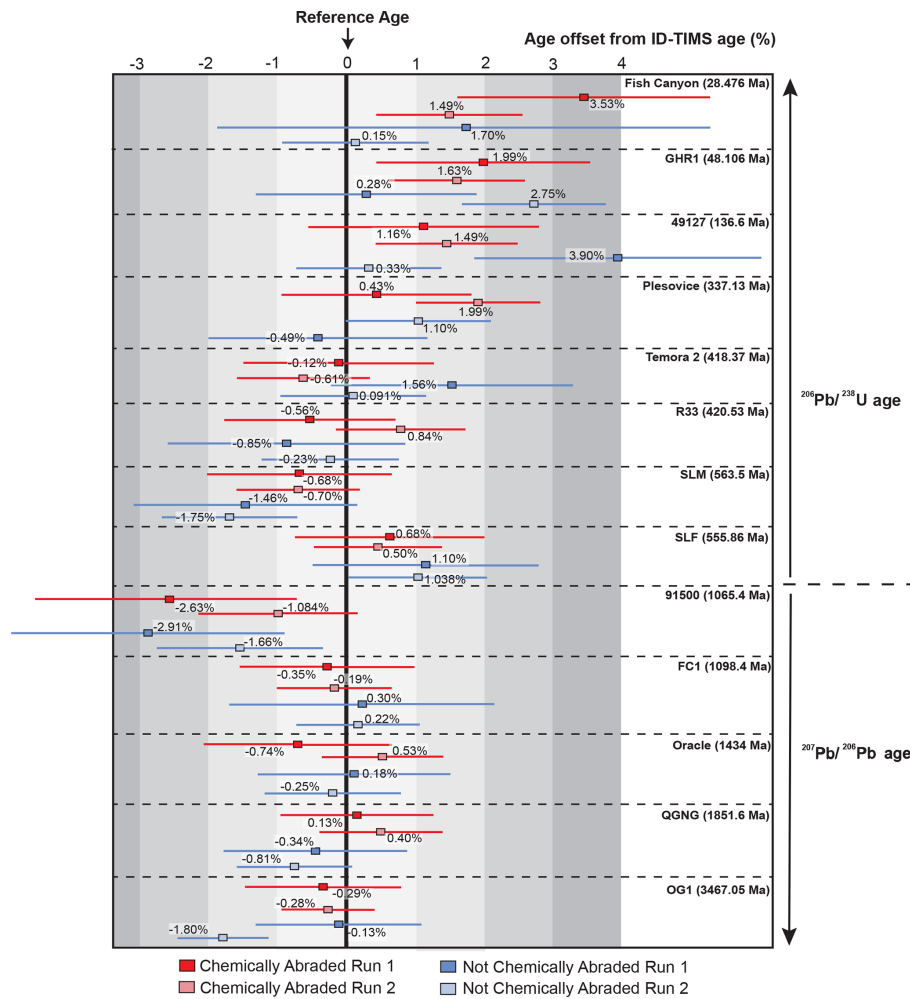


Figure 1. Comparison of $^{206}\text{Pb}/^{238}\text{U}$ and $^{207}\text{Pb}/^{206}\text{Pb}$ (CA)-LA-ICP-MS ages with CA-ID-TIMS ages for 13 reference materials that range in age from 28 to 3467 Ma. Each square is the weighted mean of a set of (CA)-LA-ICP-MS measurements shown as the percent offset from the known reference age (ID-TIMS). The uncertainty is reported as 2σ standard error of the weighted mean. Chemical abrasion of treated aliquots was conducted at Purdue University and laser ablation analyses were conducted at Arizona LaserChron Center on the Thermo Element2 single-collector ICP-MS. Methods for LA-ICP-MS at LaserChron using the Element2 are described by Pullen et al. (2018).

direct result of differences in zircon matrices and are known as “matrix effects” (Marillo-Sialer et al., 2016). Differences in zircon matrices are related to numerous factors (see review in Marillo-Sialer et al., 2016), including the presence or absence of trace elements (Black et al., 2004), the amount of radiation damage (Allen and Campbell, 2012), and the degree of crystallinity (Steely et al., 2014). These factors all impact the laser’s ability to couple with the surface of the zircon, directly impacting laser ablation rates and the rates of down-hole fractionation. As a result, matrix effects can lead to systematic shifts in LA-ICP-MS data and may be a contributor to observed shifts in treated and untreated aliquots of reference materials in this study (Fig. 1). In order to constrain how CA impacts laser coupling and ablation rates between treated and untreated reference materials, we ablated 10 spots on a single treated and untreated zircon crystal of FC1, SL, and

R33 ($n = 60$; Table S14). For each individual spot 1–10 on a reference material, we incrementally raised the ablation duration by 3 s (i.e., by 21 individual laser pulses at 7 Hz). This resulted in 10 different spots with ablation durations ranging from 3 to 30 s (21 to 210 laser pulses) and allowed us to calculate laser ablation rates for both treated and untreated zircon. Overall, laser ablation rates varied linearly with time (0.43 to $0.46 \mu\text{m s}^{-1}$) and were similar for treated and untreated aliquots of all primary reference materials (Fig. 2). Similar ablation rates were observed across all three different treated and untreated aliquots of primary reference materials. This suggests that (1) the primary reference materials have similar zircon matrix densities and ablate at similar rates (Marillo-Sialer et al., 2014, 2016), and (2) chemical abrasion does not change the zircon matrix density or alter the zircon

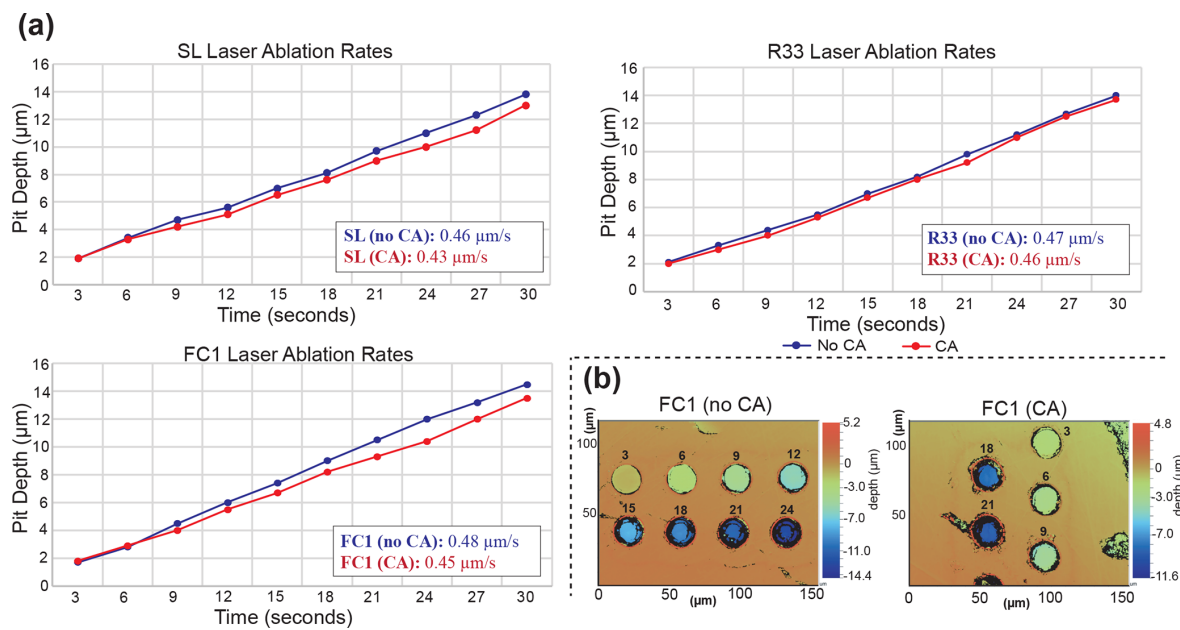


Figure 2. (a) Line graphs showing pit depths (μm) versus time (seconds) for unabraded and abraded aliquots of primary reference materials. Each data point represents an individual pit. Untreated reference materials have slightly deeper pit depths and ablate at marginally faster rates, but overall, rates of ablation for treated and untreated reference materials are similar. (b) An example of one of the Veeco surface data maps showing pit depths on treated and untreated zircon of FC1. Pits are labeled with the duration in seconds of ablation. See Table S14 for all pit depth data from abraded and unabraded reference materials.

surface of primary reference materials in a way that drastically alters laser coupling or ablation rates.

3.2 Untreated and CA U–Pb zircon LA-ICP-MS analyses of metamict zircon

A Precambrian granite sample from the Parguaza Complex in the northern Guiana Shield (MIGU-02; $5^{\circ}21'3.70''\text{N}$; $67^{\circ}41'33.41''\text{W}$) that has experienced substantial radiation damage was analyzed to assess the effects of chemical abrasion on grains with significant Pb loss. Untreated ($n = 20$) and treated aliquots ($n = 23$) of MIGU-02 were analyzed at the ALC and compared to a reference age determined by CA-ID-TIMS ($n = 6$) at Purdue University (Fig. 3; Tables S14 and S15). During the bulk chemical abrasion process, 80%–85% of MIGU-02 grains fully dissolved, leaving only a small fraction of the original aliquot to be used for analyses.

The $^{207}\text{Pb}/^{206}\text{Pb}$ CA-ID-TIMS reference age for MIGU-02 is $1394.28 \pm 1.11\text{ Ma}$ ($n = 6$, MSWD = 0.36), while the $^{206}\text{Pb}/^{238}\text{U}$ dates are more scattered (Fig. 3). The scatter indicates that U/Pb elemental fractionation occurred during chemical abrasion in one analysis (slight reverse discordance) and residual Pb loss remained in others (normal discordance) (Fig. 4). Nevertheless, a weighted-mean date of the $^{206}\text{Pb}/^{238}\text{U}$ CA-ID-TIMS dates is $1391.97 \pm 0.53\text{ Ma}$ ($n = 6$, MSWD = 11.06) and indicates that residual Pb loss only affects the dates at the $< 0.5\%$ level. Untreated LA-

ICP-MS analyses of MIGU-02 show significant discordance (Fig. 4) and only four analyses ($n = 4/20$; 80% discordant) were retained after filtering by AgeCalcML v.1.42. Chemical abrasion substantially increased the number of concordant analyses ($n = 23/23$). A total of 15 analyses were removed from the untreated aliquot dataset and 7 analyses were removed from the treated aliquot dataset because they hit epoxy and are not included in the totals. Although all grains were concordant in the treated aliquot, four grains were not included in the weighted mean because they had a significantly older $^{207}\text{Pb}/^{206}\text{Pb}$ dates (1571–1900 Ma) than the CA-ID-TIMS reference date (Table S14) and are likely xenocrystic. The weighted-mean $^{207}\text{Pb}/^{206}\text{Pb}$ date from the untreated MIGU-02 aliquot is $1353.32 \pm 13.26\text{ Ma}$ ($n = 4/20$; MSWD = 87.76) and the treated aliquot is $1395.014 \pm 4.61\text{ Ma}$ ($n = 19/23$; MSWD = 3.25). The mean $^{206}\text{Pb}/^{238}\text{U}$ date of the untreated aliquot is $1169.30 \pm 11.84\text{ Ma}$ (MSWD = 20.37) and the mean $^{206}\text{Pb}/^{238}\text{U}$ date of the treated aliquot is $1388.86 \pm 3.69\text{ Ma}$ (MSWD = 3.20). Thus, the dates from treated zircon show a significant increase in concordance, precision, and accuracy relative to the reference date as determined by CA-ID-TIMS (Fig. 3).

All the CA-treated analyses have lower ^{238}U beam intensity than the untreated grains, suggesting that CA selectively removed zones of higher U concentration (Fig. 5). Furthermore, the untreated zircons with the highest ^{238}U beam intensity are associated with U–Pb dates that are $> \pm 20\%$ discordant.

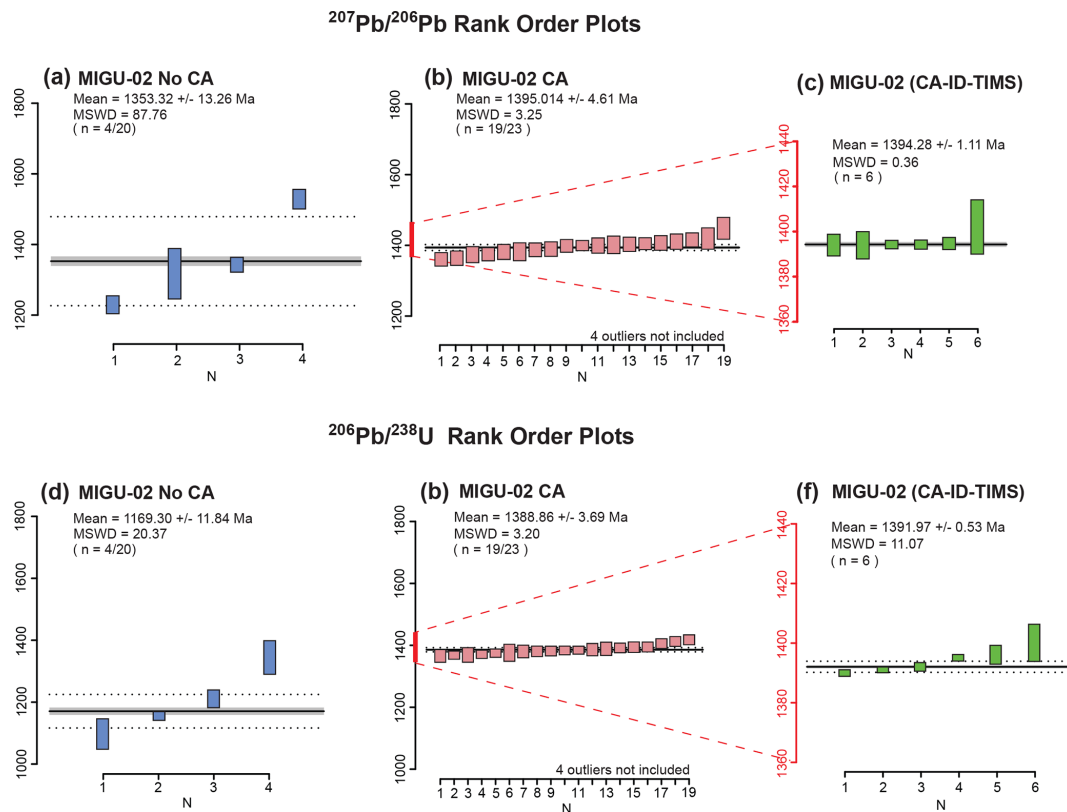


Figure 3. Rank order plots of calculated $^{207}\text{Pb}/^{206}\text{Pb}$ and $^{206}\text{Pb}/^{238}\text{U}$ ages for treated and untreated MIGU-02 aliquots and of the reference age for MIGU-02 obtained using CA-ID-TIMS. (a) Untreated samples of MIGU-02 show a large degree of scatter in dates and substantial deviation from the reference age. (b) Treated zircons show a significant increase in precision and accuracy of ages relative to the reference age. (c) Reference age for MIGU-02 determined using the weighted mean of six grains. See text for discordance criteria.

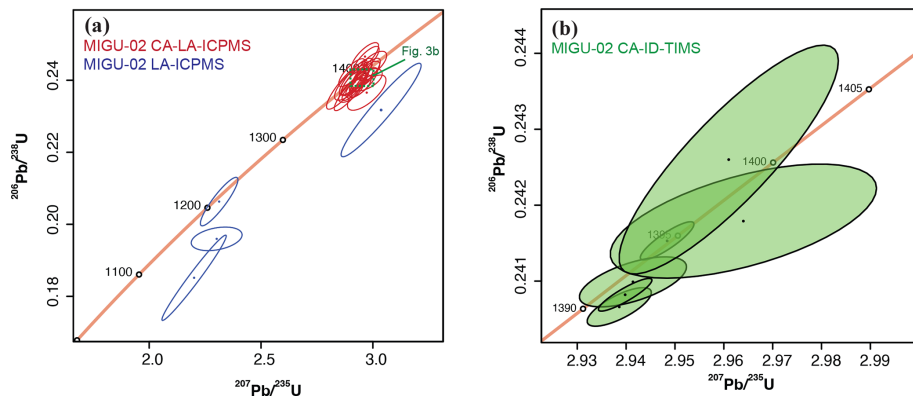


Figure 4. (a) Untreated and treated aliquots of MIGU-02 shown on a concordia plot. Non-CA MIGU-02 dates are discordant, whereas CA dates fall on concordia and overlap the reference age. (b) All CA-ID-TIMS analyses of MIGU-02 shown on a concordia plot. One date shows slight reverse discordance, whereas all other dates fall on concordia or have slight normal discordance.

dant (Table S16). Since uranium concentration is correlated with radiation damage in old zircon, this result reinforces the observation that CA is an effective tool for removing damaged zones of the zircon (Nasdala et al., 2005; Widmann et al., 2019). Pit depths were measured on five untreated and three treated zircons from MIGU-02 (Table S15). The aver-

age pit depth for untreated grains of MIGU-02 is $\sim 10.34\text{ }\mu\text{m}$, whereas it is $\sim 8.1\text{ }\mu\text{m}$ for the treated aliquot. This indicates that the pit depths of the untreated aliquot of MIGU-02 are $\sim 25\%$ deeper than the treated aliquot and that CA does have an impact on the laser ablation rate in highly metamict samples.

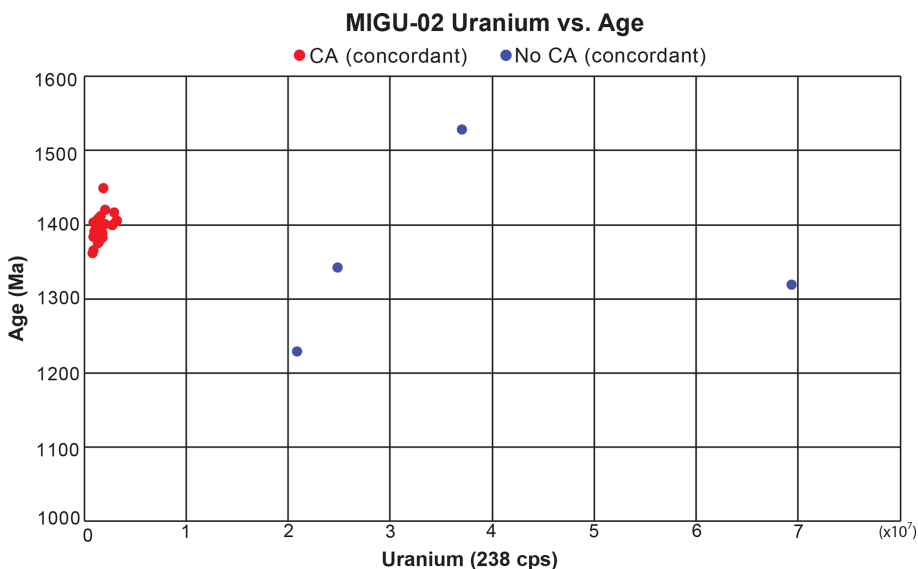


Figure 5. Uranium (238 cps) plotted against $^{207}\text{Pb}/^{206}\text{Pb}$ age (Ma) for both treated and untreated aliquots of MIGU-02. Only concordant analyses are shown because discordant analyses for MIGU-02 have extremely low ^{238}U cps. Uranium concentration is directly proportional to radiation damage in zircon with the same low-temperature cooling history. The restricted range of low ^{238}U cps in the CA-treated grains suggests that CA was effective at dissolving high-U zircon that was more likely to have Pb loss.

We acknowledge that for samples with significant radiation damage, there is always the possibility that the entire sample will dissolve during chemical abrasion, and it is up to the researcher to determine if this technique is appropriate for their objectives. Running a high- n data acquisition on highly damaged zircon might ultimately yield enough concordant analyses to make a confident age determination, but analyses of MIGU-02 that passed typical discordance filters were inaccurate by up to -11% for the $^{207}\text{Pb}/^{206}\text{Pb}$ dates and -21% for the $^{206}\text{Pb}/^{238}\text{U}$ dates (Fig. 3), suggesting that even filtered data may be inaccurate for metamict zircon. In contrast, the chemically abraded aliquot did not have these issues, despite the significant loss of zircon grains during the HF chemical attack.

3.3 Untreated and CA U–Pb zircon LA-ICP-MS analyses of detrital zircon

One Phanerozoic (NM8A) and one Precambrian sample (Rora Med) were analyzed to determine how detrital zircon age distributions compare between chemically abraded and untreated aliquots. We followed the “large- n ” approach of Pullen et al. (2014) for both treated and untreated aliquots to obtain a more robust distribution of ages, their modes, peak widths, and abundances. For NM8A, we analyzed 512 individual zircons in the treated aliquot and 896 zircons in the untreated aliquot. In Rora Med, we analyzed 1035 zircons in the treated aliquot and 920 zircons in the untreated aliquot. We used the Saylor and Sundell (2016) DZstats program to complete a quantitative assessment of the similarity between treated and untreated aliquots (see definitions de-

scribed above; Table S22). Additionally, we calculated the fraction of grains that defined distinct peak age populations in each aliquot to assess how the proportion of each population changed after chemical abrasion. Our results show that chemical abrasion (CA) changed the number and distribution of apparent peak age populations in both DZ samples compared to the non-CA age spectra (Figs. 6 and 7). Most notably, the Phanerozoic age peaks in sample NM8A narrowed, became more defined, and, in some cases, shifted to slightly older dates.

In the Precambrian sample (Rora Med), there are subtle changes in the DZ age spectra between the treated and untreated aliquots. Overall, the CA treated aliquot shows a higher percentage of concordant grains (Fig. 6), narrower and better-defined peak age populations, changes in the number of peaks present, and a slight but noticeable shift in peak age populations to older ages (Fig. 6). Of note is that the 1890 Ma peak narrows in the treated aliquot compared to the broad peak that covers a range of ages between 1890 and 2000 Ma in the untreated aliquot. However, the fraction of grains within this population decreased from 7.6 % to 3.5 % between the untreated and treated fractions, respectively. There is also a change in the shape and number of peaks between the two fractions between 2100 and 2300 Ma. In the untreated aliquot, there are three distinct peak age populations (~ 2120 Ma, $\sim 7.9\%$; ~ 2190 Ma, $\sim 4.5\%$; ~ 2260 Ma, $< 2\%$), whereas in the treated aliquot, there is only one broad peak age population that spans between ~ 2120 and 2190 Ma ($\sim 30\%$). There is also a distinct shift in the untreated aliquot 2675 Ma peak age population to 15 million years older in the treated aliquot (Fig. 6). Quantitative comparisons support

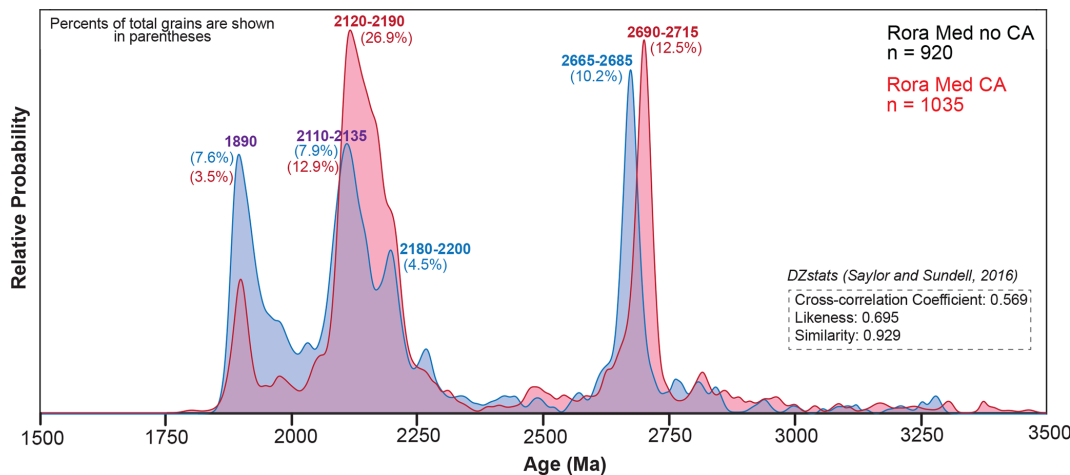


Figure 6. Comparison of U–Pb detrital zircon age spectra of non-chemically-abraded (blue) and chemically abraded (red) aliquots of Rora Med. Areas where age spectra overlap are shaded in purple. Quantitative comparisons of treated and untreated aliquots were completed using Saylor and Sundell (2016) DZstats to calculate cross-correlation, likeness, and similarity values. All quantitative comparison analytics are reported in Table S20. The percentages above the peaks represent the percentage the peak age population represents out of the total grains. We aimed for $n = 1000$ for each aliquot because Pullen et al. (2014) show that the distribution of analyzed zircon ages is thought to approach the “true” age distribution of the sample.

these observations. A likeness coefficient of 0.695 and cross-correlation coefficient of 0.569 support the fact that there are significant differences in the number, shape, and magnitude of certain peak age populations. However, a similarity value of 0.929 indicates that even with these changes for specific age populations, there is an overall high degree of overlap in the number and proportion of modes in the detrital zircon spectra between treated and untreated aliquots.

There are also subtle changes in the number of peaks and peak shapes between the treated and untreated aliquots of NM8A. The most significant changes observed are increased resolution and definition of Phanerozoic peak age populations in the treated aliquot (Fig. 7). For example, between 200 and 300 Ma, two broad peaks in the untreated aliquot sharpen and narrow to two well-defined peak age populations in the treated aliquot (Fig. 7b). Additionally, a distinct 190 Ma peak is present in the treated aliquot compared to a broad range of populations between 160 and 210 Ma in the untreated aliquot. We also see a zone of two broadly defined peaks at 68 and 72 Ma in the untreated aliquot sharpen to a singular peak at 69 Ma in the treated aliquot. In the untreated aliquot, the 68–72 Ma age populations make up $\sim 1.2\%$ of the total grains in the untreated aliquot, whereas in the treated aliquot the 69 Ma peak age population represents $\sim 1.3\%$ of total grains. There is also an older shift from the 93 Ma peak in the untreated aliquot to ~ 98 Ma in the treated aliquot. However, due to the low number of grains within these peak age populations, it is possible that these shifts are related to subtle differences between the two fractions and not a consequence of the chemical abrasion process. For example, the peak height change in the 93 Ma population (three grains; untreated aliquot) to the 98–100 Ma (four grains; treated

aliquot) represents the addition of a single grain (Fig. 7c). Other shifts and changes in peak age populations that are < 120 Ma (Fig. 7c) cannot be confidently constrained due to the low number of analyses that define those populations (one to two grains). The fraction of concordant grains is indistinguishable between treated and untreated aliquots of NM8A (Fig. 8). Quantitative comparisons of treated and untreated aliquots further support these results, and similarity, cross-correlation, and likeness values are all > 0.8 (Fig. 6). The similarity value of 0.957 indicates a strong overlap in the number and proportion of detrital zircon peak age populations overall. Slightly lower, but still high, cross-correlation (0.851) and likeness (0.816) coefficients support minor shifts in the number of peak age populations (modes) and changes in peak heights (magnitude).

4 Discussion

Our study shows that chemical abrasion prior to LA-ICP-MS analysis does not negatively affect resulting U–Pb dates provided that chemically abraded reference materials are used as the primary reference material for calibration (e.g., Crowley et al., 2014; von Quadt et al., 2014). We also show that chemical abrasion is extremely effective in mitigating the effects of Pb loss in LA-ICP-MS U–Pb dating of zircon that has experienced substantial radiation damage. Significant improvement was observed in both $^{206}\text{Pb}/^{238}\text{U}$ and $^{207}\text{Pb}/^{206}\text{Pb}$ dates of MIGU-02 zircon relative to ID-TIMS results, and also the efficiency of the analyses was dramatically improved by focusing LA-ICP-MS analyses on only those grains and/or fragments that survived the chemical

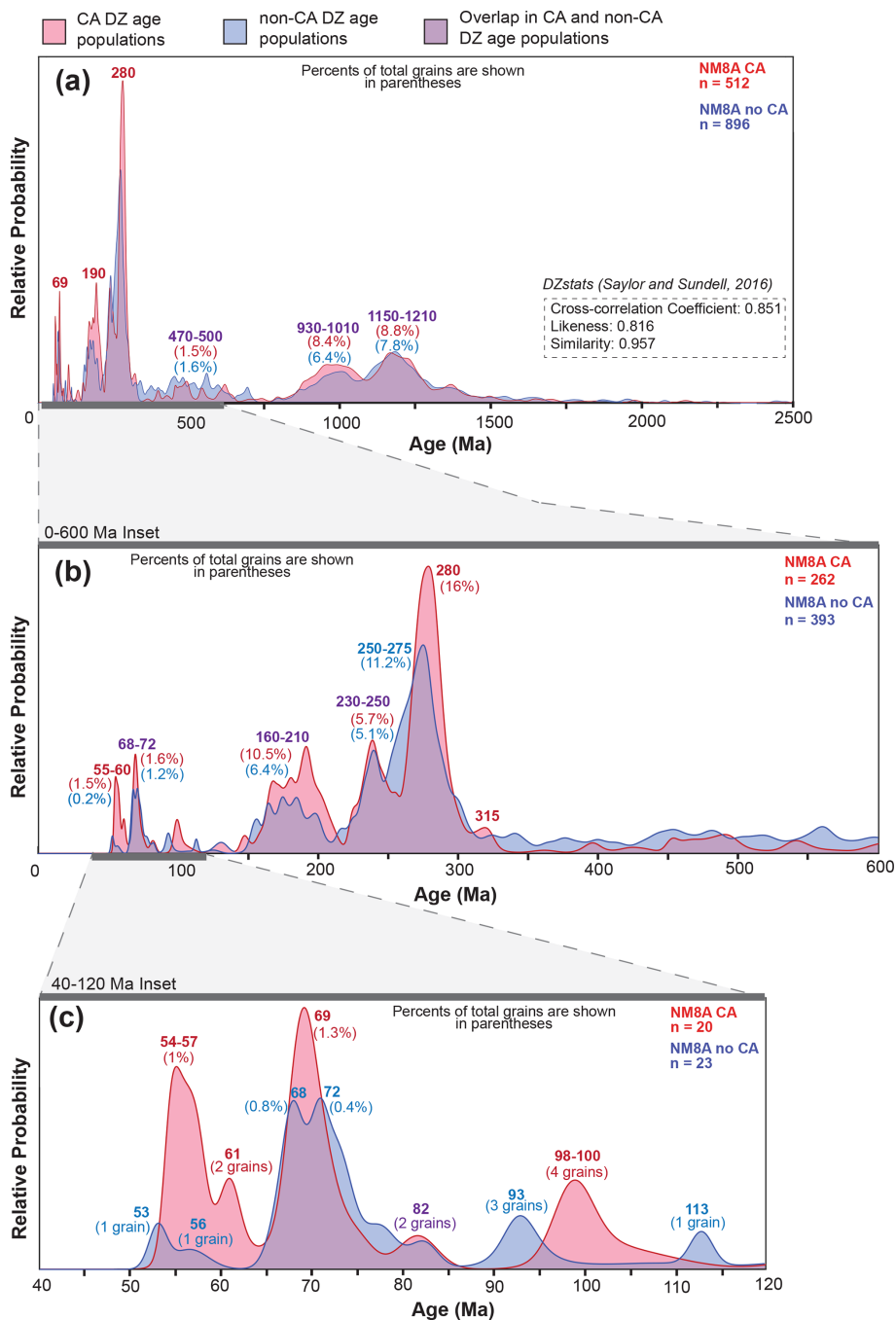


Figure 7. Comparison of U–Pb detrital age spectra of non-chemically-abraded (blue) and chemically abraded (red) aliquots of NM8A. Areas where age spectra overlap are shaded in purple. Quantitative comparisons of treated and untreated aliquots were completed using Saylor and Sundell (2016) DZstats to calculate cross-correlation, likeness, and similarity values. All quantitative comparison analytics are reported in Table S20. The percentages above the peaks represent the percentage the peak age population represents out of the total grains. We aimed for $n = 1000$ for each aliquot as the distribution of analyzed zircons ages is thought to approach the “true” age distribution of the sample (Pullen et al., 2014). Panels (a)–(c) show variations of the scale on the x axis.

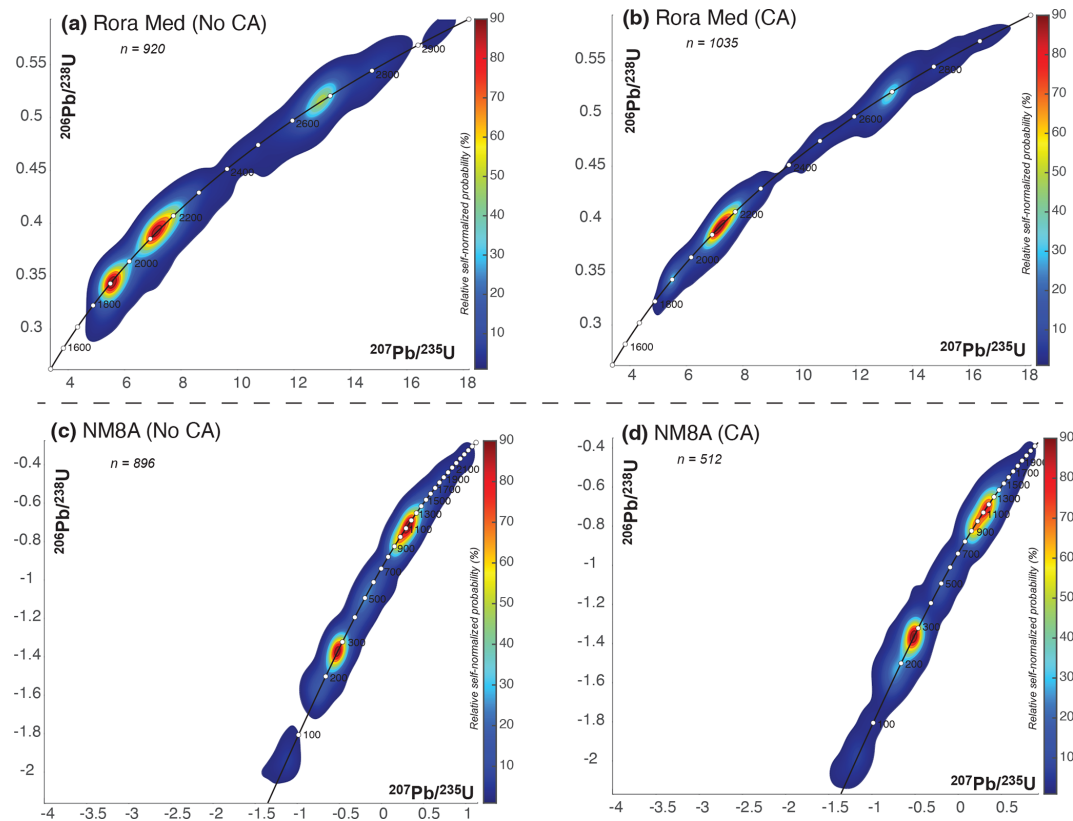


Figure 8. Density contour concordia diagrams for non-chemically-abraded and chemically abraded aliquots of detrital zircon samples NM8A and Rora Med (a–d). There is substantial improvement in the scatter of concordant analyses in the chemically abraded aliquot of the Proterozoic Rora Med sample compared to the untreated aliquot (a–b). However, both aliquots of the Phanerozoic NM8A sample are indistinguishable (c–d). Please note that the concordia diagrams for NM8A (c–d) are plotted on a logarithmic scale to best display the large range of Phanerozoic to Precambrian ages.

abrasion process and had not sustained significant radiation damage. These results reinforce the observations of previous studies that used this approach (Crowley et al., 2014; von Quadt et al., 2014) and suggest that the CA-LA-ICP-MS method can be valuable for studies that need increased precision and accuracy in LA-ICP-MS U–Pb zircon analyses, although care must be taken to ensure data are not biased when this pre-treatment is applied.

One important consideration is whether chemical abrasion negatively affects the laser ablation process. Variations in laser ablation pit depths have been directly correlated with the density of the zircon matrix (Marillo-Sialer et al., 2014, 2016), and changes in ablation rate change down-hole fractionation. Previous research has indicated that annealing leads to lower ablation rates compared to unannealed zircon and more homogenous rates across annealed zircon with variable initial degrees of radiation damage (Marillo-Sialer et al., 2016). These observations support results from Allen and Campbell (2012) that thermal annealing of zircon samples prior to LA-ICP-MS will reduce matrix-related bias and improve accuracy and precision. However, the impact of CA on laser coupling and ablation rates is not as well charac-

terized. Crowley et al. (2014) found that treated zircons had pit depths that were 25 % shallower than untreated aliquots of zircons that experienced extensive Pb loss. This is identical to the results for the metamict MIGU-02 sample in this study in which chemically abraded zircon also had ~ 25 % shallower ablation pits than untreated zircon (Table S15). The shallower pit depths could be driven by less effective laser coupling in treated aliquots due to small-scale etching and creation of a 3-D porous texture by partial dissolution (Crowley et al., 2014). In comparison, laser ablation rates and pit depths in treated and untreated aliquots of primary reference materials were nearly identical (Fig. 2). This supports conclusions drawn by Crowley et al. (2014) that the extent to which zircon is impacted by CA is dependent on U concentration and the presence of physical defects and highlights the importance of incorporating a wide range chemically abraded reference materials in each analytical session.

Our data, and the data of Crowley et al. (2014) and von Quadt et al. (2014), indicate that, provided that care is taken to use chemically abraded reference materials, the pre-treatment will mitigate Pb loss and lead to increased accuracy in LA-ICP-MS U–Pb zircon analyses. Given this ap-

parent benefit, it is natural to extend the technique to detrital zircon and test the advantages and disadvantages afforded by this method. Crowley et al. (2014) first used this approach on an Archean graywacke and showed that it did not significantly bias their results. However, this technique has not been widely used over the last decade. We report similar results to previous studies in that chemical abrasion does not significantly bias results or negatively affect LA-ICP-MS dates. This is supported by quantitative comparison tests of the treated and untreated aliquots of both detrital zircon samples that show high degrees of similarity between aliquots. Minor changes in cross-correlation and likeness values are a result of minor changes in the number and magnitude of specific peak age populations between treated and untreated aliquots (Figs. 6 and 7). Our results indicate that a chemical abrasion pre-treatment may help resolve finer-scale features in detrital zircon spectra from the Cenozoic to the Archean. We attribute this increased resolution mainly to the mitigation of Pb loss, leading to increased accuracy of the resulting LA-ICP-MS U–Pb dates.

The mitigation of Pb loss is most clearly observed in the sharpening of Neoproterozoic through Cenozoic age populations because $^{206}\text{Pb}/^{238}\text{U}$ dates provide the most precise estimate for zircon crystallization in this age range. Pb loss can significantly affect the accuracy of dates in this age range since Pb loss trajectories closely follow concordia and can result in dates that have apparent concordance despite being inaccurate. These effects can be seen most clearly in sample NM8A where age peaks narrowed and became more defined (e.g., 250–300 Ma peak age populations) following chemical abrasion and some peak age populations shifted to slightly older dates (Fig. 7). Assuming that the zircons that form these populations cooled below the temperature at which radiation damage is effectively annealed at a similar time, then U content can be used as a proxy for radiation damage (Nasdala et al., 2005; Widmann et al., 2019; McKenna et al., 2023). This is clearly observed for the treated and untreated aliquots of igneous sample MIGU-02, where the treated aliquot has substantially lower ^{238}U beam intensities and increased concordance and accuracy in $^{206}\text{Pb}/^{238}\text{U}$ dates (Figs. 3, 4, and 5). However, the thermal history is not known *a priori* for detrital zircon datasets, meaning this same assessment applied to NM8A and Rora Med is more uncertain.

To examine whether the reduced Pb loss we observed in the chemically abraded aliquot reflects the selective dissolution of zircon with radiation damage, we compared zircon ^{238}U beam intensity from a particular age range (250–320 Ma) in NM8A as a first-order approximation (Fig. 9). We assume that the populations in this range likely have the same low- T history, although this assumption cannot be tested with our data. We also note that these populations showed the most significant sharpening following chemical abrasion (Fig. 7b). Figure 9 shows that the average ^{238}U beam intensity of treated grains in this age range is similar, but there is a distinct proportion of treated grains that have lower ^{238}U

intensities. This supports our interpretation that CA is likely mitigating Pb loss by dissolving zircon with high U concentrations and that this process can be observed by the changes in the number of peaks, their shape, and their magnitude between treated and untreated aliquots. These changes are especially apparent when comparing the shift and change in magnitude of the Rora Med 2665–2685 Ma (untreated aliquot) peak age to 2690–2715 Ma (treated aliquot).

Reduced Pb loss in Mesoproterozoic and older zircon also benefits detrital zircon studies because ancient Pb loss can bias $^{207}\text{Pb}/^{206}\text{Pb}$ dates of moderately discordant or even (analytically) concordant zircon toward erroneously young values (Nemchin and Cawood, 2005). This effect has led many laboratories to filter for discordance within their datasets. Thus, improving concordance will increase the proportion of dates that can be retained in a detrital zircon study and improve confidence in the identification of peak age populations. One potential issue with this approach is the possibility that entire zircon populations could be removed during chemical abrasion if they have high degrees of radiation damage. Surprisingly, we did not see this effect in either NM8A or Rora Med. This result is surprising and may be sample-specific, since Rora Med zircons from all age populations have low ^{238}U beam intensities (Fig. 10b). Although our Rora Med sample did not entirely lose any age populations during CA, changes in the magnitude of peak heights suggests preferential dissolution of some age populations associated with Pb loss. This feature may be unique to Precambrian samples with overall low zircon U concentrations and/or recent exhumation of the sedimentary rocks to the temperature conditions where radiation damage can accumulate and Pb loss occurs. Regardless, both NM8A and Rora Med have similarity values of > 0.9 (Figs. 6 and 7), indicating that similar peak age populations and proportions are present in both treated and untreated aliquots. Therefore, it is unlikely that chemical abrasion would impact detrital zircon spectra in a way that would make aliquots look as though they were sampling different source terranes.

The nature of sediment transport may also work to remove metamict zircon prior to deposition in certain environments. Hydraulic sorting, mechanical abrasion, and weathering can naturally bias detrital zircon populations present in a different lithologies (Malusa et al., 2013; Ibañez-Mejia et al., 2018). For example, Ewing et al. (2003) noted that metamictization leads to structural damage of the zircon crystal structure and that this can be correlated with a decrease in density and hardness. These changes lead metamict zircon to be more prone to destruction during river transport (Fedo et al., 2003; Hay and Dempster, 2009a). In particular, Hay and Dempster (2009a) argue that inclusion-rich and metamict zircon are broken during sediment transport and that these fragments do not survive being incorporated into clastic sandstone deposits. Instead, these smaller fragments can be swept out to more distal depositional environments. Small zircons are also typically lost during sample preparation (Hietpas et

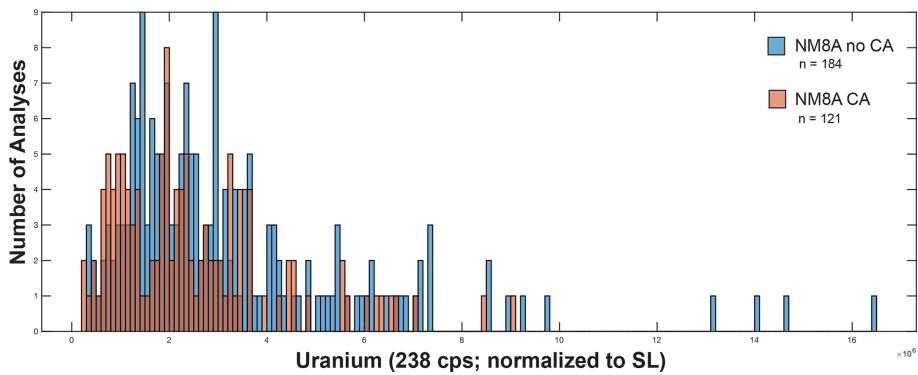


Figure 9. Histogram showing ^{238}U cps (normalized to SL) for zircons in the peak age population between 250 and 320 Ma in detrital zircon sample NM8A. On the detrital zircon spectra, this age population narrows from one broad peak in the untreated aliquot to a well-defined, narrow peak in the treated aliquot (Fig. 7b). Measured ^{238}U cps values from this peak age population of treated and untreated aliquots are overall similar, but there is a distinguishable proportion of grains in the treated aliquot that have lower ^{238}U cps.

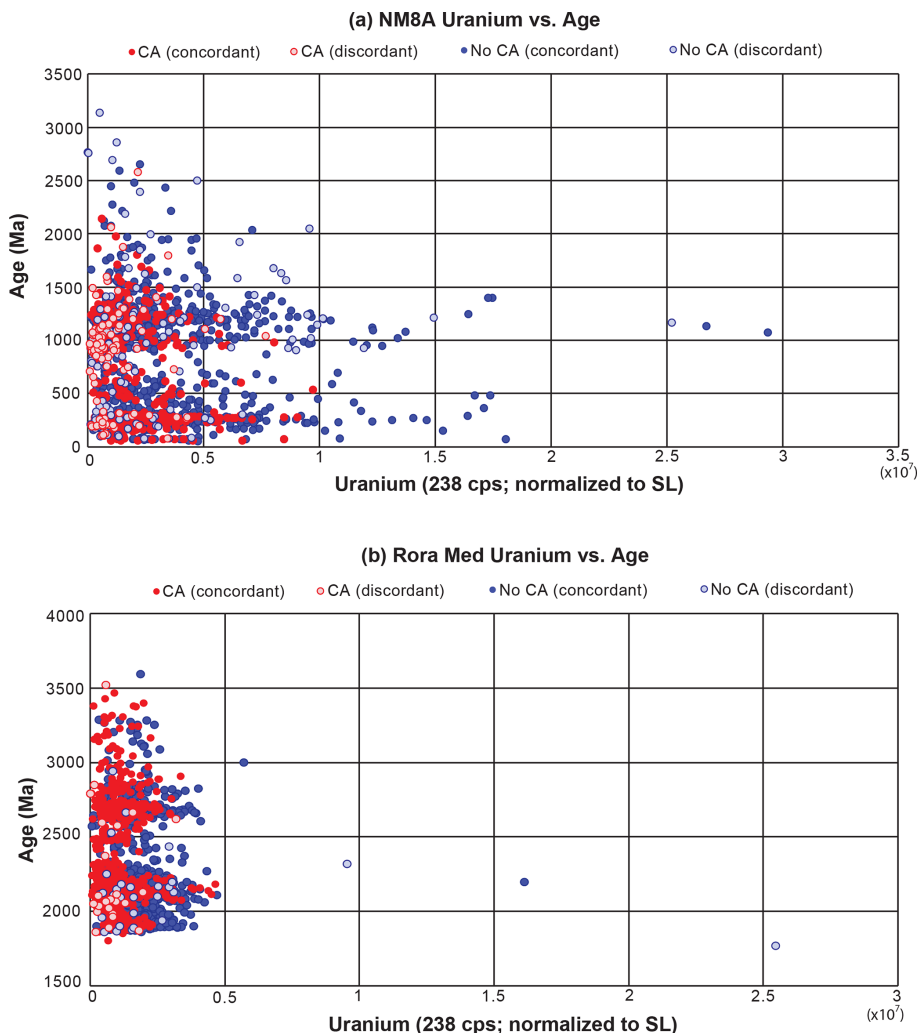


Figure 10. Scatter plot of ^{238}U cps (normalized to SL) plotted against the age (Ma) for both treated and untreated aliquots of (a) NM8A and (b) Rora Med. Both concordant and discordant analyses are shown. Overall, CA appears to effectively reduce scatter in ^{238}U cps in all age populations compared to the untreated aliquot but most significantly reduces scatter in Precambrian ages.

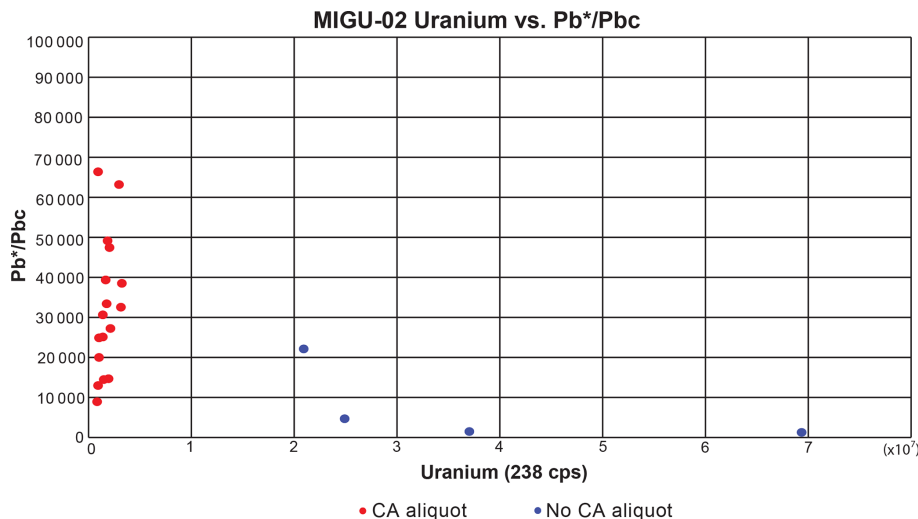


Figure 11. Pb^*/Pb_c ratios are plotted against ^{238}U cps for MIGU-02. The Pb^*/Pb_c ratios in the treated aliquot of MIGU-02 are significantly higher than the untreated aliquot for similar concentrations of U. Higher Pb^*/Pb_c ratios in the treated aliquot of MIGU-02 can be attributed to reduction of Pb_c by removal of inclusions.

al., 2011; Sláma and Kosler, 2012), meaning that both natural and laboratory processes may preferentially lead to a high proportion of undamaged zircon in sandstone samples. Thus, while we did not observe the removal of specific age populations following chemical abrasion in the two detrital zircon samples that were analyzed in this study, and there are reasons to suspect that natural and laboratory processes will favor the analysis of undamaged zircon anyway, we recognize that other samples may behave differently. Future users of this technique should carefully consider this possibility in their datasets.

Another potential benefit of chemical abrasion is the preferential dissolution of inclusions within zircon during the partial dissolution step (McKenna et al., 2023). Inclusions harbor Pb_c that can be incorporated into the analyzed volume during laser ablation, reducing the Pb^*/Pb_c and limiting measurement precision and accuracy. When comparing the Pb^*/Pb_c ratios of treated and untreated aliquots of MIGU-02, we see a clear distinction in that treated zircons have a much higher Pb^*/Pb_c ratio for similar ranges in ^{238}U beam intensity (Fig. 11). We note that the overall ^{238}U beam intensities for the treated aliquot of MIGU-02 are low compared to the untreated aliquot, as we have already shown that CA for metamict zircon effectively removes high-U zones where Pb loss is most likely to have occurred (see above discussion; Fig. 5). Regardless, the increased Pb^*/Pb_c ratio for the treated aliquot of MIGU-02 shows that this method is also efficient in removing inclusions with high Pb_c content and/or highly damaged domains where Pb_c might have been introduced by fluids. These two effects are correlated with an increased fraction of concordant grains as well as increased precision and accuracy in $^{206}\text{Pb}/^{238}\text{U}$ zircon dates in the chemically abraded aliquot. These observations support

the benefits of utilizing CA prior to LA-ICP-MS measurements in metamict igneous zircon suites. A comparison of the Pb^*/Pb_c ratios in treated and untreated aliquots of detrital samples (Fig. S18) shows similar behavior in Rora Med with slightly higher Pb^*/Pb_c in the treated aliquot and no change in the Pb^*/Pb_c ratios in NM8A. We conclude that it is likely that CA is removing inclusions prior to analysis of detrital zircons as well. However, it is difficult to isolate this effect since detrital zircons are sourced from various terranes and we cannot confidently compare the Pb^*/Pb_c of zircon with the same age, U concentration, and thermal history.

5 Conclusions and recommended applications

Chemical abrasion is a widely used tool in the zircon U–Pb ID-TIMS community (see reviews in Schoene, 2014; Schaltegger et al., 2015), where it has been repeatedly shown to mitigate the negative effects on age accuracy introduced by Pb loss (Mundil et al., 2004; Mattinson, 2005; Widmann et al., 2019). Recent efforts to extend chemical abrasion to LA-ICP-MS analyses have also shown that this pre-treatment can be beneficial (Crowley et al., 2014; Von Quadt et al., 2014; McKenna et al., 2023; Sharman and Malkowski, 2023). The extension of this pre-treatment to large-*n* detrital zircon analyses is a natural outgrowth of these efforts. Our results indicate no negative effects from chemical abrasion prior to LA-ICP-MS analyses and that the technique results in improved percentages of concordant grains, reduced uncertainty, and, at least for the highly radiation damaged igneous sample we studied here, accuracy of measured U–Pb dates. For DZ samples, these benefits appear to translate to more defined and slightly older $^{206}\text{Pb}/^{238}\text{U}$ age peaks for Phanerozoic zircon, more concordant analyses, and in some cases slightly

older $^{207}\text{Pb}/^{206}\text{Pb}$ dates for Precambrian zircon. One potential drawback of this pre-treatment is the possibility that age populations characterized by high-U zircon may be selectively dissolved during chemical abrasion. We did not observe this effect in either of our tested samples. However, we remain wary of its possibility in other samples with highly damaged Precambrian zircon populations, so future practitioners are advised to proceed with caution. The differences between age distributions in our analyzed detrital zircon spectra are slight and indicate that the Pb loss present in typical untreated analyses would not significantly alter the interpretation of sediment source terranes at a broad scale. However, chemical abrasion did sharpen several Phanerozoic peak ages and led to an increased percentage of concordant grains in Precambrian zircon populations. This indicates that the pre-treatment may be useful in certain scenarios in which researchers may require increased resolution of detrital zircon age spectra to distinguish fine-scale variations in provenance, sediment source terranes, or source characteristics. Ongoing research aims to test this method's impact on improving the precision and accuracy of maximum depositional age (MDA) estimations.

Data availability. All datasets utilized in this study are available in the Supplement.

Supplement. The supplement related to this article is available online at: <https://doi.org/10.5194/gchron-6-89-2024-supplement>.

Author contributions. EED, MPE, and MIM all helped design experiments for treated and untreated zircon aliquots, and EED prepared all bulk chemically abraded aliquots and conducted CA-ID-TIMS experiments. FM and EED both conducted LA-ICP-MS and CA-LA-ICP-MS experiments. FM and MIM designed and FM conducted zircon optical profilometry experiments. All authors participated in the interpretation and discussion of results. EED prepared the figures and paper.

Competing interests. The contact author has declared that none of the authors has any competing interests.

Disclaimer. Publisher's note: Copernicus Publications remains neutral with regard to jurisdictional claims made in the text, published maps, institutional affiliations, or any other geographical representation in this paper. While Copernicus Publications makes every effort to include appropriate place names, the final responsibility lies with the authors.

Acknowledgements. We thank the Arizona LaserChron Center (ALC) for sharing samples and reference materials and for help-

ing analyze these samples. Specifically, we thank George Gehrels, Mark Pecha, Dan Alberts, Wai Allen, Michelle Foley, and Tom Milder. We also thank Ryan Ickert for help designing a system for bulk CA at Purdue. This paper has benefited from the thoughtful comments of reviewers David M. Chew, Trystan Herriott, Matthew Horstwood, and Marcel Guillong, as well as the associate editor Daniela Rubatto and editor Klaus Mezger.

Financial support. All LA-ICPMS measurements were made at the Arizona LaserChron Center under NSF-EAR 2050246 for support of the Arizona LaserChron Center, and all CA steps and CA-ID-TIMS measurements were completed at Purdue University's Radiogenic Isotope Geology Lab (RIGL) under NSF-EAR-2151277 to Michael P. Eddy.

Review statement. This paper was edited by Daniela Rubatto and reviewed by David M. Chew, Marcel Guillong, and Matthew Horstwood.

References

Allen, C. M. and Campbell, I. H.: Identification and elimination of a matrix-induced systematic error in LA-ICP-MS $^{206}\text{Pb}/^{238}\text{U}$ dating of zircon, *Chem. Geol.*, 323–333, 157–165, 2012.

Anderson, T.: Detrital zircons as tracers of sedimentary provenance: limiting conditions from statistics and numerical simulation, *Chem. Geol.*, 216, 249–270, <https://doi.org/10.1016/j.chemgeo.2004.11.013>, 2005.

Bateman, H.: Solution of a system of differential equations occurring in the theory of radioactive transformations, *P. Camb. Philos. Soc.*, 15, 423–427, 1910.

Black, L. P.: Recent Pb loss in zircon: a natural or laboratory-induced phenomenon?, *Chem. Geol.*, 65, 25–33, 1987.

Black, L. P., Kamo, S. L., Allen, C. M., Davis, D. W., Aleinikoff, J. N., Valley, J. W., Mundil, R., Campbell, I. H., Korsch, R. J., Williams, I. S., and Foudoulis, C.: Improved $^{206}\text{Pb}/^{235}\text{U}$ microprobe geochronology by the monitoring of a trace-element-related matrix effect; SHRIMP, ID-TIMS, ELA-ICP-MS and oxygen isotope documentation for a series of zircon standards, *Chem. Geol.*, 205, 115–140, <https://doi.org/10.1016/j.chemgeo.2004.01.003>, 2004.

Bowring, J. F., McLean, N. M., and Bowring, S. A.: Engineering cyber infrastructure for U–Pb geochronology: Tripoli and U–Pb redux, *Geochem. Geophys. Geosy.*, 12, Q0AA19, <https://doi.org/10.1029/2010GC003479>, 2011.

Carrapa, B.: Resolving tectonic problems by dating detrital minerals, *Geology*, 38, 191–192, <https://doi.org/10.1130/focus022010.1>, 2010.

Chakoumakos, B. C., Murakami, T., Lumpkin, G. R., and Ewing, R. C.: Alpha-decay induced fracturing in zircon: The transition from the crystalline to metamict state, *Science*, 236, 1556–1559, 1987.

Condon, D. J., Schoene, B., McLean, N. M., Bowring, S. A., and Parrish, R. R.: Metrology and traceability of U–Pb isotopic dilution geochronology (EARTHTIME tracer calibration part 1), *Geochim. Cosmochim. Ac.*, 164, 464–480, 2015.

Coutts, D. S., Matthews, W. A., and Hubbard, S. M.: Assessment of widely used methods to derive depositional ages from detrital zircon populations, *Geosci. Front.*, 10, 1421–1435, 2019.

Crowley, Q. G., Heron, K., Riggs, N., Kamber, B., Chew, D., McConnell, B., and Benn, K.: Chemical Abrasion Applied to LA-ICP-MS U-Pb Zircon Geochronology, *Minerals*, 4, 503–518, <https://doi.org/10.3390/min4020503>, 2014.

Dickin, A. P.: *Radiogenic Isotope Geology*, 2nd Edn., Cambridge University Press, Cambridge, UK, <https://doi.org/10.1017/CBO9781139165150>, 2005.

Dickinson, W. R. and Gehrels, G. E.: Use of U-Pn ages of detrital zircons to infer maximum depositional ages of strata: a test against a Colorado Plateau Mesozoic database, *Earth Planet. Sc. Lett.*, 288, 115–125, 2009.

Eddy, M. P., Ibañez-Mejia, M., Burgess, S. D., Coble, M. A., Cordani, U. G., DesOrmeau, J., Gehrels, G. E., Li, X., MacLennan, S., Pecha, M., Sato, K., Schoene, B., Valencia, V. A., Vervoort, J. D., and Wang, T.: GHR1 Zircon – A New Eocene Natural Reference Material for Microbeam U-Pb Geochronology and Hf Isotopic Analysis of Zircon, *Geostand. Geoanal. Res.*, 43, 113–132, <https://doi.org/10.1111/ggr.12246>, 2019.

Ewing, R. C., Meldrum, A., Wang, L., Weber, W. J., and Corrales, I. R.: Radiation effects in zircon, in: *Zircon. Rev. Mineral. Geochem.*, edited by: Hanchar, J. M. and Hoskin, P. W. O., 53, Mineral Society of America, 277–303, <https://doi.org/10.2113/0530387>, 2003.

Fedo, C. M., Sircombe, K., and Rainbird, R.: Detrital zircon analysis of the sedimentary record, *Rev. Mineral. Geochem.*, 53, 277–303, <https://doi.org/10.2113/0530277>, 2003.

Garver, J. I. and Kamp, P. J. J.: Integration of zircon color and zircon fission track zonation patterns in orogenic belts: Application of Southern Alps, New Zealand, *Tectonophysics*, 349, 203–219, 2002.

Gehrels, G. E.: Detrital zircon U-Pb geochronology: current methods and new opportunities, in: *Tectonics of Sedimentary Basins: Recent Advances*, edited by: Busby, C. and Azor, A., 47–62, Chichester, UK, Wiley-Blackwell, <https://doi.org/10.1002/9781444347166.ch2>, 2012.

Gehrels, G. E.: Detrital zircon U-Pb Geochronology Applied to Tectonics, *Annu. Rev. Earth Planet. Sc.*, 42, 127–149, <https://doi.org/10.1146/annurev-earth-050212-124012>, 2014.

Gehrels, G. E., Valencia, V., and Ruiz, J.: Enhanced precision, accuracy, efficiency, and spatial resolution of U-Pb ages by laser ablation–multicollector–inductively coupled plasma–mass spectrometry, *Geochem. Geophys. Geosyst.*, 9, Q03017, <https://doi.org/10.1029/2007GC001805>, 2008.

Gehrels, G. E., Rusmore, M., Woodsworth, G., Crawford, M., Andronicos, C., Hollister, L., and Patchett, J.: U-Th-Pb geochronology of the Coast Mountains batholith in north-coastal British Columbia: Constraints on age and tectonic evolution, *Geol. Soc. Am. Bull.*, 121, 1341–1361, 2009.

Ginster, U., Reiners, P. W., Nasdala, L., and Chanmuang, C. N.: Annealing kinetics of radiation damage in zircon, *Geochim. Cosmochim. Ac.*, 15, 225–246, 2019.

Goldich, S. S. and Mudrey Jr., M. G.: Dilatancy model for discordant U-Pb zircon ages, in: *Contributions to Recent Geochemistry and Analytical Chemistry (Vinogradov Volume)*, edited by: Tugarinov, A. I., PASCAL, PASCALGEODEBRGM7720087455, 415–418, 1972.

Hay, D. C. and Dempster, T. J.: Zircon alteration, formation, and preservation in sandstones, *Sedimentology*, 56, 2175–2191, <https://doi.org/10.1111/j.1365-3091.2009.01075.x>, 2009a.

Herriott, T. M., Crowley, J. L., Schmitz, M. D., Marwan, W. A., and Gillis, R. J.: Exploring the law of detrital zircon: LA-ICP-MS and CA-TIMS geochronology of Jurassic fore-arc strata, Cook Inlet, Alaska, USA, *Geology*, 47, 1044–1048, <https://doi.org/10.1130/G46312.1>, 2019.

Hiess, J., Condon, D. J., McLean, N., and Noble, S. R.: $^{238}\text{U}/^{235}\text{U}$ Systematics in Terrestrial Uranium-Bearing Minerals, *Science*, 335, 1610–1614, 2012.

Hietpas, J., Samson, S., Moecher, D., and Chakraborty, S.: Enhancing tectonic and provenance information from detrital zircon studies: assessing terrane-scale sampling and grain-scale characterization, *J. Geol. Soc. Lond.*, 168, 309–318, 2011.

Ibañez-Mejia, M., Pullen, A., Pepper, M., Urbani, F., Ghoshal, G., and Ibañez-Mejia, J. C.: Use and abuse of detrital zircon U-Pb geochronology – A case from the Rio Orinoco delta, eastern Venezuela, *Geology*, 46, 1019–1022, 2018.

Jaffey, A. H., Flynn, K. F., Glendenin, L. E., Bentley, W. C., and Essling, A. M.: Precision Measurement of Half-Life and Specific Activities of ^{235}U and ^{238}U , *Phys. Rev. C*, 4, 1889, <https://doi.org/10.1103/PhysRevC.4.1889>, 1971.

Keller, C. B., Boehnke, P., Schoene, B., and Harrison, M.: Step-wise chemical abrasion-isotope dilution-thermal ionization mass spectrometry with trace element analysis of microfractured Hadean zircon, *Geochronology*, 1, 85–97, 2019.

Kramers, J., Frei, R., Newville, M., Kober, B., and Villa, I.: On the valency state of radiogenic lead in zircon and its consequences, *Chem. Geol.*, 261, 4–11, <https://doi.org/10.1016/j.chemgeo.2008.09.010>, 2009.

Krogh, T. E.: A low-contamination method for hydrothermal decomposition of zircon and extraction of U and Pb for isotopic age determinations, *Geochim. Cosmochim. Ac.*, 87, 485–494, 1973.

Malusa, M. G., Carter, A., Limoncelli, M., Villa, I. M., and Garzanti, E.: Bias in detrital zircon geochronology and thermochronometry, *Chem. Geol.*, 359, 90–107, 2013.

Marillo-Sialer, E., Woodhead, J., Hanchar, J. M., Reddy, S. M., Greig, A., Hergt, J., and Kohn, B. P.: An investigation of laser-induced zircon “matrix effect”, *Chem. Geol.*, 438, 11–24, 2016.

Marillo-Sialer, E., Woodhead, J., Hergt, J., Greig, A., Guillong, M., Gleadow, A., Evans, N., and Paton, C.: The zircon “matrix effect”: evidence for an ablation rate control on the accuracy of U-Pb age determinations by LA-ICP-MS, *J. Anal. Atom. Spectrom.*, 29, 981–989, 2014.

Marsellos, A. E. and Garver, J. J.: Radiation damage and uranium concentration in zircon as assessed by Raman spectroscopy and neutron irradiation, *Am. Mineral.*, 95, 1192–1201, 2010.

Mattinson, J. M.: A study of complex discordance in zircons using step-wise dissolution techniques, *Contrib. Mineral. Petr.*, 116, 117–129, 1994.

Mattinson, J. M.: Zircon U-Pb chemical-abrasion (“CA-TIMS”) method: Combined annealing and multi-step dissolution analysis for improved precision and accuracy of zircon ages, *Chem. Geol.*, 220, 47–56, <https://doi.org/10.1016/j.chemgeo.2005.03.011>, 2005.

Mattinson, J. M.: Analysis of the relative decay constants of ^{235}U and ^{238}U by multi-step CA-TIMS measurements of closed

system natural zircon samples, *Chem. Geol.*, 275, 186–198, <https://doi.org/10.1016/j.chemgeo.2010.05.007>, 2010.

McKenna, A. J., Koran, I., Schoene, B., and Ketcham, R. A.: Chemical abrasion: the mechanics of zircon dissolution, *Geochronology*, 5, 127–151, <https://doi.org/10.5194/gchron-5-127-2023>, 2023.

McLean, N. M., Condon, D. J., Schoene, B., and Bowring, S. A.: Evaluating uncertainties in the calibration of isotopic reference materials and multi-element isotopic tracers (EARTHTIME tracer calibration II), *Geochim. Cosmochim. Ac.*, 164, 481–501, 2015.

Mundil, R., Ludwig, K. R., Metcalfe, I., and Renne, P. R.: Age and timing of the Permian mass extinctions: U/Pb dating of closed-system zircons, *Science*, 305, 1760–1763, <https://doi.org/10.1126/science.1101012>, 2004.

Nasdala, L., Hanchar, J. M., Kronz, A., and Whitehouse, M. J.: Long-term stability of alpha particle damage in natural zircon, *Chem. Geol.*, 220, 83–103, <https://doi.org/10.1016/j.chemgeo.2005.03.012>, 2005.

Nemchin, A. and Cawood, P.: Discordance of the U-Pb system in detrital zircons: Implication for provenance studies of sedimentary rocks, *Sediment. Geol.*, 182, 143–162, 2005.

Pullen, A., Ibañez-Mejia, M., Gehrels, G. E., Ibanez-Mejia, J. C., and Pecha, M.: What happens when $n = 1000$? Creating large- n geochronological datasets with LA-ICP-MS for geologic investigations, *J. Anal. Spectrom.*, 29, 971–980, <https://doi.org/10.1039/C4JA00024B>, 2014.

Pullen, A., Ibañez-Mejia, M., Gehrels, G. E., Giesler, D., and Pecha, M.: Optimization of a Laser Ablation-Single Collector-Inductively Coupled Plasma-Mass Spectrometer (Thermo Element 2) for Accurate, Precise, and Efficient Zircon U-Th-Pb Geochronology, *Geochem. Geophys. Geosy.*, 19, 3689–3705, 2018.

Reiners, P. W.: Zircon (U-Th)/He Thermochronometry, *Rev. Mineral. Geochem.*, 58, 151–179, 2005.

Satkoski, A. M., Wilkinson, B. H., Hietpas, J., and Samson, S. D.: Likeness among detrital zircon populations – An approach to the comparison of age frequency data in time and space, *Geol. Soc. Am. Bull.*, 125, 1783–1799, 2013.

Saylor, J. E. and Sundell, K. E.: Quantifying comparison of large detrital geochronology data sets, *Geosphere*, 12, 1–18, 2016.

Schaltegger, U., Schmitt, A. K., and Horstwood, M. S. A.: U-Th-Pb zircon geochronology by ID-TIMS, SIMS, and laser ablation ICP-MS: recipes, interpretations, and opportunities, *Chem. Geol.*, 402, 89–110, <https://doi.org/10.1016/j.chemgeo.2015.02.028>, 2015.

Schmitz, M. D. and Bowring, S. A.: U-Pb zircon and titanite systematics of the Fish Canyon Tuff: an assessment of high-precision U-Pb geochronology and its application to young volcanic rocks, *Geochim. Cosmochim. Ac.*, 65, 2571–2587, 2001.

Schoene, B.: U-Th-Pb Geochronology, Treatise on geochemistry, 2nd Edn., edited by: Rudnick, R., Elsevier, <https://doi.org/10.1016/B978-0-08-095975-7.00310-7>, 2014.

Sharman, G. R. and Malkowski, M. A.: Needles in a haystack: Detrital zircon U-Pb ages and the maximum depositional age of modern global sediment, *Earth Sci. Rev.*, 203, <https://doi.org/10.1016/j.earscirev.2020.103109>, 2020.

Sharman, G. R. and Malkowski, M. A.: Modeling apparent Pb loss in zircon U-Pb geochronology, *Geochronology*, 6, 37–51, 2023.

Smith, T. M., Saylor, J. E., Lapen, T. J., Leary, R. J., and Sundell, K. E.: Large detrital zircon data set investigation and provenance mapping: Local versus regional and continental sediment sources before, during, and after Ancestral Rocky Mountain deformation, *GSA Bulletin*, 135, 2901–2921, <https://doi.org/10.1130/B36285.1>, 2023.

Sláma, J. and Kosler, J.: Effects of sampling and mineral separation on accuracy of detrital zircon studies, *Geochem. Geophys. Geosy.*, 13, Q05007, <https://doi.org/10.1029/2012GC004106>, 2012.

Sláma, J., Kosler, J., Condon, D. J., Crowley, J. L., Gerdes, A., Hanchar, J. M., Horstwood, M. S. A., Morris, G. A., Nasdala, L., Norberg, N., Schaltegger, U., Schoene, B., Tubrett, M. N., and Whitehouse, M. J.: Plesovice zircon – A new natural reference material for U-Pb and Hf isotopic microanalysis, *Chem. Geol.*, 249, 1–35, <https://doi.org/10.1016/j.chemgeo.2007.11.005>, 2008.

Steely, A. N., Hourigan, J. K., and Juel, E.: Discrete multi-pulse laser ablation depth profiling with a single-collector ICP-MS: Sub-micron U-Pb geochronology of zircon and the effect of radiation damage on depth-dependent fractionation, *Chem. Geol.*, 372, 92–108, 2014.

Stern, R. A., Bodorkos, S., Kama, S. L., Hickman, A. H., and Corfu, F.: Measurement of SIMS instrumental mass fractionation of Pb isotopes during zircon dating, *Geostand. Geoanal. Res.*, 33, 145–168, <https://doi.org/10.1111/j.1751-908X.2009.00023.x>, 2009.

Sundell, K. E., Gehrels, G. E., and Pecha, M. E.: Rapid U-Pb Geochronology by Laser Ablation Multi-Collector ICP-MS, *Geostand. Geoanal. Res.*, 45, 37–57, 2021.

Vermeesch, P.: Maximum depositional age estimation revisited, *Geosci. Front.*, 12, 843–850, 2021.

Von Quadt, A., Dallhofer, D., Guilong, M., Peytcheva, I., Waelle, M., and Sakata, S.: U-Pb dating of CA/non-CA treated zircons obtained by LA-ICP-MS and CA-TIMS techniques: impact for their geological interpretation, *J. Anal. Atom. Spectrom.*, 29, 1618–1629, <https://doi.org/10.1039/C4JA00102H>, 2014.

Wang, J. W., Gehrels, G., Kapp, P., and Sundell, K.: Evidence for regionally continuous Early Cretaceous sinistral shear zones along the western flank of the Coast Mountains, coastal British Columbia, Canada, *Geosphere*, 19, 139–162, 2022.

Widmann, P., Davies, J. H. F. L., and Schaltegger, U.: Calibrating chemical abrasion: Its effects on zircon crystal structure, chemical composition and U-Pb age, *Chem. Geol.*, 511, 1–10, <https://doi.org/10.1016/j.chemgeo.2019.02.026>, 2019.

Wiedenbeck, M., Alle, P., Corfu, F., Griffin, W. L., Meier, M., Oberli, F., von Quadt, A., Roddick, J. C., and Spiegel, W.: Three natural zircon standards for U-Th-Pb, Lu-Hf, trace element and REE analyses, *Geostandard. Newslett.*, 19, 1–23, 1995.

Wotzlaw, J. F., Schaltegger, U., Frick, D. A., Dungan, M. A., Gerdes, A., and Gunther, D.: Tracking the evolution of large-volume silicic magma reservoirs from assembly to supereruption, *Geology*, 41, 867–870, 2013.